

Evaluation of Recursive PIV Algorithm with Correlation Based Correction Method Using Various Flow Images

Daichin, Sang Joon Lee*

Department of Mechanical Engineering, Pohang University of Science and Technology, San 31, Hyoja-Dong, Nam gu, Pohang, Kyungbuk 790-784, Korea

The hierarchical recursive local-correlation PIV algorithm with CBC (correlation based correction) method was employed to increase the spatial resolution of PIV results and to reduce error vectors. The performance of this new PIV algorithm was tested using synthetic images, PIV standard images of Visualization Society of Japan, real flows including ventilation flow inside a vehicle passenger compartment and wake behind a circular cylinder with riblet surface. As a result, most spurious vectors were suppressed by employing the CBC method, the hierarchical recursive correlation algorithm improved the sub-pixel accuracy of PIV results by decreasing the interrogation window size and increased spatial resolution significantly. However, with recursively decreasing of interrogation window size, the SNR (signal-to-noise ratio) in the correlation plane was decreased and number of spurious vectors was increased. Therefore, compromised determination of optimal interrogation window size is required for given flow images, the performance of recursive algorithm is also discussed from a viewpoint of recovery ratio and error ratio in the paper.

Key Words : Recursive Correlation Algorithm, CBC (Correlation Based Correction), PIV, Performance Test

Nomenclature

Φ_r : Recovery ratio
 Φ_e : Error ratio
 D_m : Maximum particle displacement
 N : Particle numbers
 D : Diameter of circular cylinder
 X : Distance from circular cylinder in horizontal
 Re : Reynolds number
 ρ_N : Particle density

1. Introduction

The conventional PIV algorithms widely used in nowadays are based on statistic correlation of

particle images, i.e. auto-correlation for single-frame multiple exposure images or cross-correlation for double-frame single-exposure particle images. These correlation algorithms divide each single image into a number of sub-regions, so-called interrogation windows. For each interrogation window the correlation function is calculated and the position of displacement peak is determined on the correlation plane. Then, the representative velocity of the interrogation window is determined by dividing the displacement value by time interval between two exposures. Since the displacement peak obtained by the spatial correlation method represents the average movement of particles in each interrogation window, the spatial resolution of vector field measured by a PIV technique is directly related with size of interrogation window. If the interrogation window is large enough and covers some small-scale turbulent structures or vortex structures, all these detailed flow information might be lost

* Corresponding Author,

E-mail : sjlee@postech.ac.kr

TEL : +82-54-279-2169; FAX : +82-54-279-3199

Professor, Department of Mechanical Engineering, Pohang University of Science and Technology, San 31, Hyoja-Dong, Nam gu, Pohang, Kyungbuk 790-784, Korea. (Manuscript Received January 30, 2002; Revised November 19, 2002)

during the PIV correlation analysis and adjacent velocity vectors may not be continuous. Furthermore, the differential quantities from the velocity information, such as vorticity, will be limited by spatial resolution of velocity field. In addition, the derived vorticity is a local average of the already spatial-averaged velocity field and the magnitude of vorticity may be smaller than the actual value. In order to achieve reliable velocity and vorticity data in high spatial resolution, the size of interrogation window should be decreased as small as possible.

However, Keane & Adrian (1990) mentioned that at least ten-tracing particle images were needed in each individual interrogation window to obtain accurate estimation of average displacement for the conventional PIV algorithm based on the correlation analysis. This limitation should be fulfilled by choosing a interrogation window size to have adequate number of particles in each window. With this restriction, it is difficult to improve spatial resolution of vector field significantly by decreasing the interrogation window size for conventional correlation PIV techniques. In recent years, some new algorithms for improving the spatial resolution of PIV results (Super-resolution PIV) using hierarchical recursive operation were proposed by Hart (1999), Scarnano & Riethmuller (1999, 2001), and Hu et al. (2000) Rohály et al. (2001) developed a similar algorithm named as reverse hierarchical PIV processing, however, it started to process the PIV images at the smallest interrogation window size and gradually built up the correlation planes into larger interrogation window based on the results of inter-level correlation correction and validation. Hart (2000) adopted the CBC (Correlation Based Correction) algorithm together with the recursive correlation scheme to eliminate spurious vectors in PIV results, Park and Kim (2001) employed the recursive algorithm to enhance the spatial resolution of cinematic PIV system.

In this paper, we employed the hierarchical recursive correlation algorithm with CBC processing and window offset to both single-frame and double-frame cross-correlation PIV systems. In addition, its performance was tested for vari-

ous PIV images including synthetic particle images, standard PIV images, and real flow images.

2. Hierarchical Recursive Correlation Algorithm and CBC

2.1 Hierarchical recursive correlation

The concept of the hierarchical recursive correlation algorithm is very simple. If basic information of the magnitude and direction of local displacement in the sub-region of a particle image is available, the size of the sub-region can be reduced and offset by following prediction of prior local displacement information. The in-plane loss of pairs caused by out-of-boundary particle motion can then be compensated during correlation operation. This procedure can be recursively conducted to reduce the sub-region size hierarchically, the spatial resolution of vector field is therefore increased.

We implemented the following steps to accomplish the hierarchical recursive PIV correlation operation :

- a) Carry out a conventional PIV correlation routine for an usual interrogation window in which sufficient number of particles are involved so that prominent SNR (signal to noise ratio) can be obtained on the correlation plane, perform peak detection and get displacement information for each interrogation window.
- b) Store the resulting displacement information to be used as a predictor in the further coming steps.
- c) Divide the interrogation window to half-sized regions following one quarter rule as shown in Fig. 1. Predict the offset of smaller interrogation windows using the estimated displacement data obtained from the prior step to compensate the in-plane loss of pairs caused by out-of-boundary particle motion (Fig. 2).
- d) Perform the correlation operation for smaller interrogation windows. The resulting values in this step must be added with corresponding predictor value and then produce sub-pixel displacement with higher accuracy.

Repeat the steps from (b) to (d) until getting a proper spatial resolution in the PIV results.

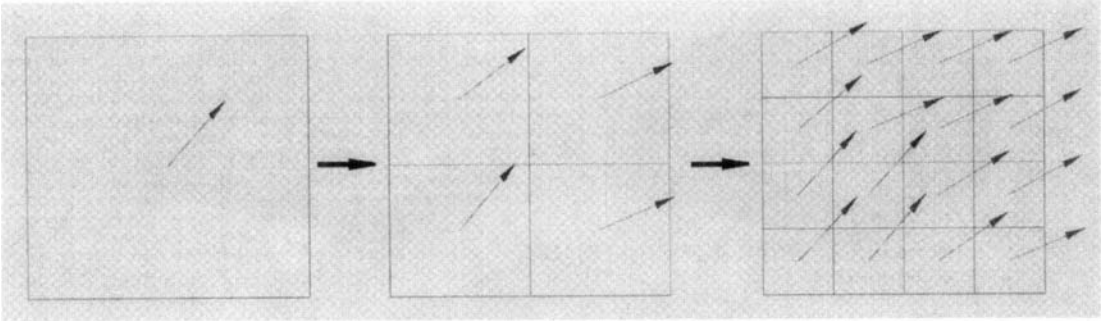


Fig. 1 Schematic of hierarchical recursive algorithm

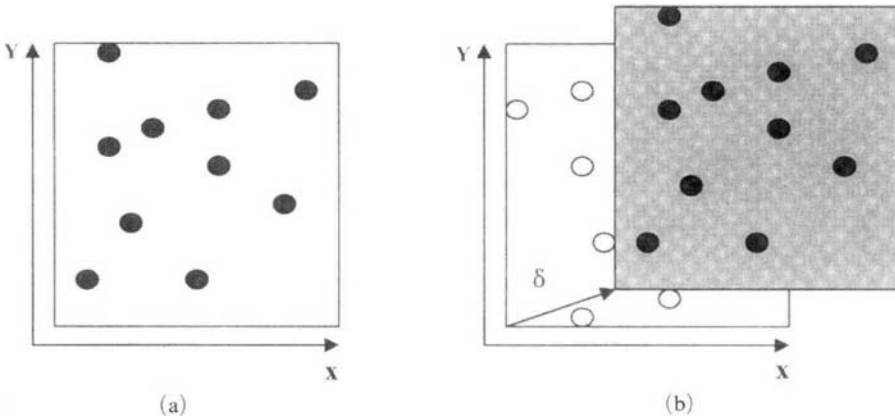


Fig. 2 Principle of interrogation window offset

2.2 Correlation based correction (CBC)

If the number of particles inside an interrogation window is insufficient at the first step of the hierarchical recursive method, the SNR (signal-noise ratio) will be very poor on the correlation plane. This may cause a displacement peak to merge in the random background noise. It is difficult to detect the displacement peak in this case and some spurious vectors may appear. Supposing this inaccurate displacement information are used to predict the offset of smaller interrogation windows in the succeeding steps, more error vectors will be generated. In general, the conventional PIV method employs an interpolation scheme to replace these spurious vectors during post-processing.

Hart (2000) proposed the CBC (correlation based correction) concept and it showed good performance in eliminating error vectors caused by anomalies in correlation. The CBC method is

based on the principle of element-by-element multiplication of correlation planes of two or more adjacent interrogation windows to improve the SNR on the multiplied correlation plane. Figure 3 illustrates the procedure of CBC method. The correlation plane 1 from the first interrogation region is multiplied by correlation plane 2 from an adjacent interrogation region which is 50% overlapped with the first interrogation region. The SNR is quite low in both of correlation planes 1 and 2, but a prominent displacement peak is observed on the multiplied correlation plane. The correlation anomalies are remarkably reduced and the error vectors can be easily eliminated before the velocity vectors are determined.

The basic idea of CBC technique is that locations of noise peaks on a correlation plane are always random, but the positions of displacement peaks are almost identical on the correlation

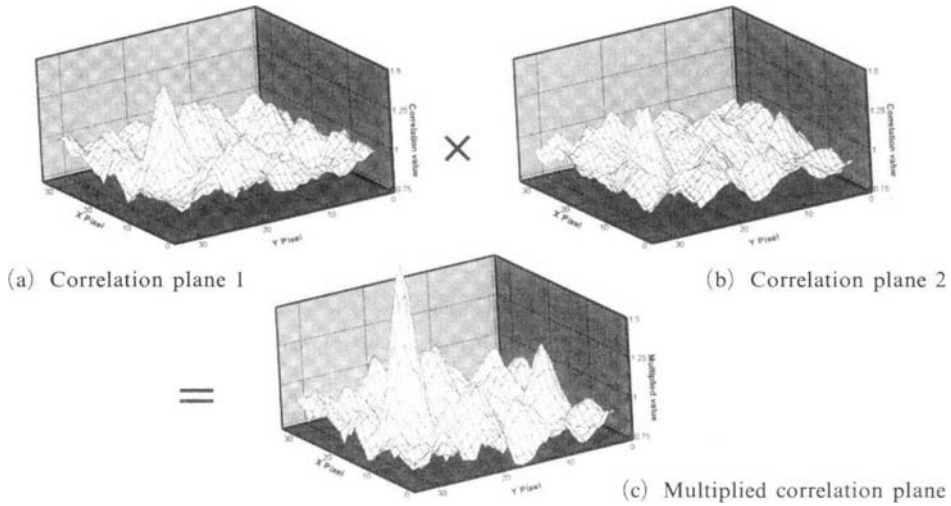


Fig. 3 Principle of CBC algorithm

planes of adjacent interrogation windows, after multiplication of the two correlation planes, the peaks of the back ground noise keep the same level as on the individual correlation planes, but the magnitude of displacement peak is increased prominently. The efficiency of reducing anomalies errors during CBC processing increases as the size of overlapped region decreases. However, the optimum overlapping depends on the flow structure of testing and the particle seeding density. In general, 50% overlapping has been adopted in most correlation algorithms. Hart (2000) mentioned that 50% overlapping was a proper value to evaluate the performance of CBC algorithm and we also conducted 50% overlapping rate in the performance test.

3. Performance Tests and Discussion

We applied the hierarchical recursive algorithm with CBC method to the cross-correlation PIV program for both single-frame and double-frame particle images. The performance tests included evaluation of efficiency of CBC for analyzing real flow image, accuracy assessment and recovery/error ratio analysis of the recursive algorithm for synthetic particle images, comparison of standard PIV images from the Visualization Society of Japan (VSJ) with variable the interrogation windows size, and finally for real flow testing.

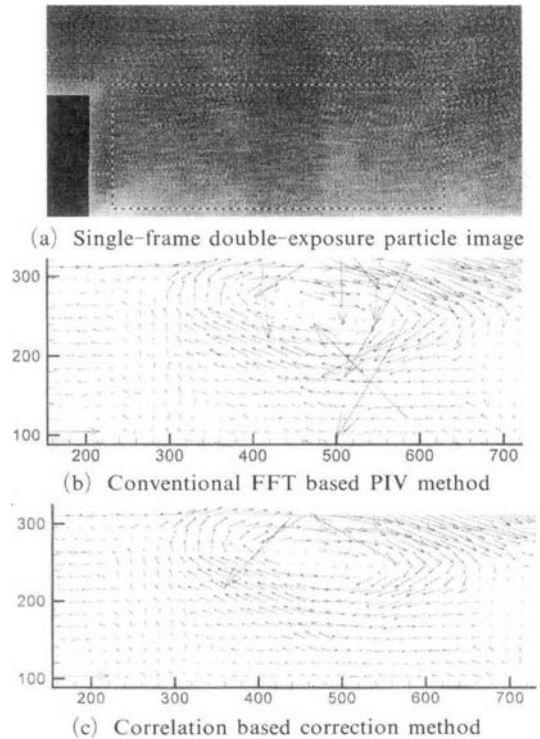


Fig. 4 Comparison of conventional FFT and CBC method for the backward facing step flow (32×32 pixels)

3.1 Efficiency of CBC processing

A single-frame double-exposure PIV particle image of backward-facing step flow was used to test the efficiency of CBC processing. The second

particle images were shifted by 9 pixels with image-shifting technique, shown in Fig. 4(a). The single-frame cross-correlation PIV technique based on conventional FFT and CBC processing were applied to the flow image with 32×32 pixels interrogation window in order to compare the number of spurious vectors in the PIV velocity field results. In Fig. 4(b), the velocity field obtained by conventional FFT based correlation method shows several error vectors. The spurious vectors have to be interpolated by proper data during post-processing, but it will not contribute to increase the sub-pixel accuracy. Figure 4(c) shows the velocity field obtained with addition of CBC processing, which multiplied correlation planes of two adjacent interrogation regions. From the result, we can see that spurious vectors are largely decreased without post-processing.

3.2 Accuracy assessment

3.2.1 RMS errors for uniform flow

There are several methods to assess the accuracy of PIV measurement results. One approach is to use particle images taken from a real flow with known quantity of particle displacement. Another commonly applied method is to use synthetic particle images generated by numerical simulation, by varying the parameters of particle images, the pre-determined displacements can be compared with the PIV result. A synthetic particle image was generated with 8-bits gray-scale randomly distributed particles. The flow image containing 4000 particles has 640×480 pixels resolution with particle diameter of 4 pixels. The second exposed particle images are imposed by a pre-set displacement (0~11 pixels) from the first particle images horizontally to simulate uniform flow.

Figure 5 shows the rms (root-mean-square errors) errors of the PIV method based on conventional FFT and hierarchical recursive PIV method as a function of particle image displacement for various interrogation window sizes. The conventional PIV results show higher rms errors due to in-plane loss of particle pairs. For the recursive PIV results, the rms errors are less than half of the rms errors of the same interrogation

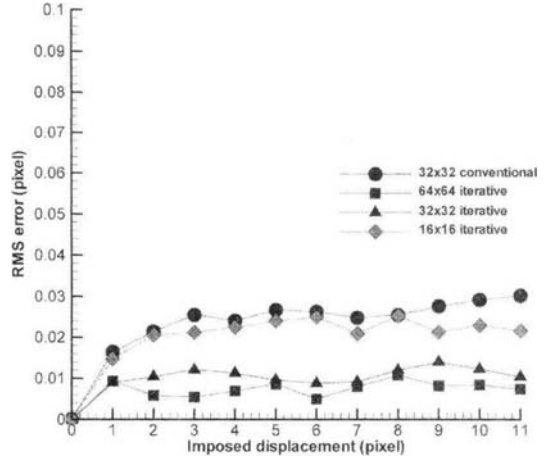


Fig. 5 Measurement RMS error as a function of particle displacement

window (hereafter mark as IW) of 32×32 pixels conventional PIV method. In addition, as the interrogation windows size increases, the RMS error is decreased. Because the seeding density is relatively sparse in this synthetic particle image, higher SNR value can not be obtained on correlation plane for 16×16 pixels interrogation window, the rms errors are lower than that of other recursive cases, but it still shows better performance compared with the conventional PIV method with 32×32 pixels IW.

3.2.2 Recovery/error ratios of solid body rotation flow and image computation time

There are many parameters affecting the accuracy of PIV algorithm. In order to investigate the effect of particle displacement to the performance of recursive algorithm, the recovery ratio Φ_r and error ratio Φ_e were calculated for specific consecutive frames with various maximum particle displacements. The recovery ratio Φ_r is defined as the ratio of the total number of accurately recovered vectors to the number of all possible vectors. The error ratio Φ_e is defined as the ratio of the number of error vectors to the total number of recovered vectors. In the study, we investigated the variations of recovery ratio and error ratio for the recursive algorithm with decreasing the interrogation window size.

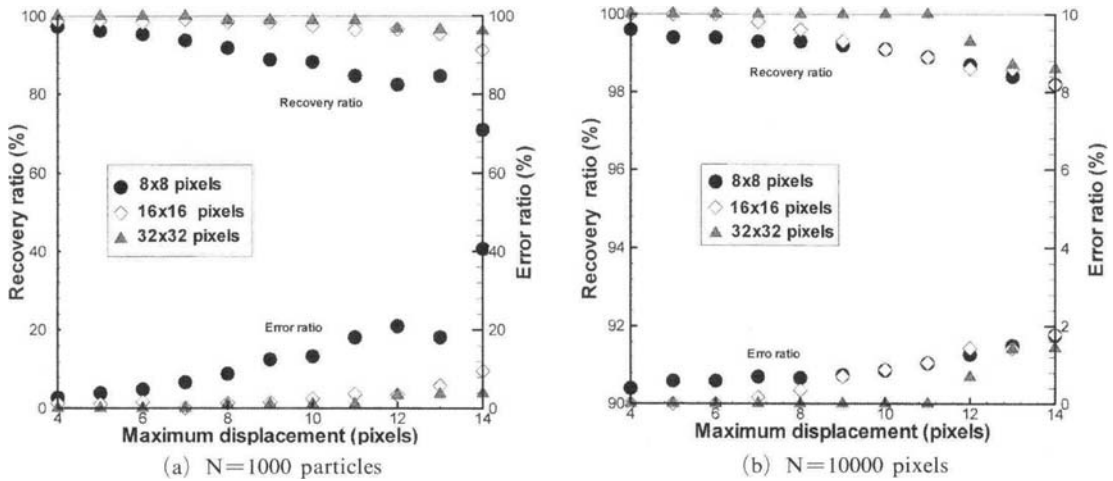


Fig. 6 Recovery/error ratio vs. maximum displacement for solid body rotation, image size : 256×256 pixels

For the performance evaluation, 22 pairs of synthetic particle images for the solid body rotation flow having different maximum displacement D_m ranged from 4 pixels to 14 pixels were tested. The maximum displacement D_m represents the displacement of particles located at the edge of the synthetic image for the solid body rotation flow. Since the solid body rotation flow has a linear velocity profile with zero velocity at the image center, if the maximum displacement is 8 pixels, for a 256×256 pixels image, the rotation angle of the flow is determined as $\tan \theta = 8 \text{ pixels} / 128 \text{ pixels}$. Each particle image has resolution of 256×256 pixels and the maximum particle diameter is 4 pixels. Figure 6(a) shows the variations of Φ_r and Φ_e as a function of maximum particle displacement D_m for images containing $N=1000$ particles, the minimum inter-particle distances are 7.5 pixels. With increase of maximum displacement, the recovery ratios Φ_r decrease and the error ratios Φ_e increase irrespective of interrogation window size. For the IW sizes of 16×16 and 32×32 pixels, recovery ratio and error ratio decrease and increase in similar trend, however, the bigger IW of 32×32 pixels shows better recovery ratio Φ_r than that of 16×16 pixels. But for 8×8 pixels IW size, variations of Φ_r and Φ_e with respect to the maximum displacement D_m are more rapid, the recovery ratio decreases from 97.3% to 71% and the maximum error ratio reaches 40%. This is caused by spar-

sely distribution of particle images, the minimum inter-particle distance (7.5 pixels) is almost as large as the IW size, so the in-plane loss of pair is inevitable. For a comparison, we estimated the recovery and error ratios for synthetic flow images with higher particle density. Figure 6(b) shows the variation of Φ_r and Φ_e for images containing $N=10000$ particles. Each flow image has spatial resolution of 256×256 pixels and the particles with diameters from 1 to 4 pixels are randomly distributed. There is few overlap of particles in the synthetic flow image, and the minimum inter-particle distance is about 2.37 pixels. In this case, even for smaller IW size of 8×8 pixels, 98.2% of recovery ratio can be obtained at 14 pixels maximum displacement. If the maximum displacement value is lower than 10 pixels, the recovery ratio Φ_r will be higher than 99%. For larger IW of 16×16 and 32×32 pixels, even higher value of recovery ratio can be obtained. The maximum error ratio for 14 pixels displacement is lower than 2% and it is less than 1% at 10 pixels maximum displacement for 8×8 pixels IW size.

We also compared the recovery ratio Φ_r and error ratio Φ_e of present algorithm with those of the two-frame PTV (Baek and Lee, 1996; Kim and Lee, 2002) for two flow images with different particle densities ρ_N (the total number of particles per unit area of flow image). The comparisons are summarized in Table. 1. In the particle image

Table 1 Comparison of recovery ratio and error ratio between the recursive PIV algorithm and two-frame PTV method

IW size (pixels)		32×32		16×16		8×8		Two frame PTV	
Max. displacement D_m (pixels)		10	5	10	5	10	5	10	5
Recovery Ratio Φ_r (%)	$\rho_N=1.5\times 10^{-2}$	98.3	100	96.9	99	88.5	97.1	92.8	97.4
	$\rho_N=1.0\times 10^{-2}$	92.7	95.6	81	89.2	69.4	76.6	94.4	99.2
Error Ratio Φ_e (%)	$\rho_N=1.5\times 10^{-2}$	1.7	0.0	3.2	1.0	12.9	3.0	7.8	2.7
	$\rho_N=1.0\times 10^{-2}$	7.9	4.6	23.3	12.1	44.1	30.5	5.9	0.8

of $\rho_N=1.5\times 10^{-2}$ ($N=1000$), the recovery and error ratios of present algorithm are 96.9% and 3.2% for 16×16 pixels IW, 88.5% and 12.9% for 8×8 pixels IW with maximum displacement of 10 pixels. The corresponding results of the two-frame PTV are between the results for 16×16 pixels IW and 8×8 pixels IW obtained with recursive PIV method. The low recovery ratio of present method at 8×8 pixels IW may be caused by the low particle density and relatively larger particle displacement. In addition, the two-frame PTV method has been known to have good performance in low particle density images, compared with other PIV/PTV techniques (Baek and Lee, (1996)). As the maximum displacement decreases to 5 pixels, the recovery ratio of recursive PIV method is increased to the same level as that of two-frame PTV method. For the case of low particle density of $\rho_N=1.0\times 10^{-2}$ ($N=660$), the recovery ratios are decreased significantly for all the IW sizes tested to the recursive PIV method. Compared with the results of two-frame PTV method, the recovery ratio is much smaller and the error ratio exceeds 30% at the smallest IW size. This indicates that the particle density of $\rho_N=1.0\times 10^{-2}$ is too low to carry out the recursive PIV processing properly. With increase of the particle density, the recovery ratio of the recursive PIV algorithm is enhanced and the error ratio is decreased.

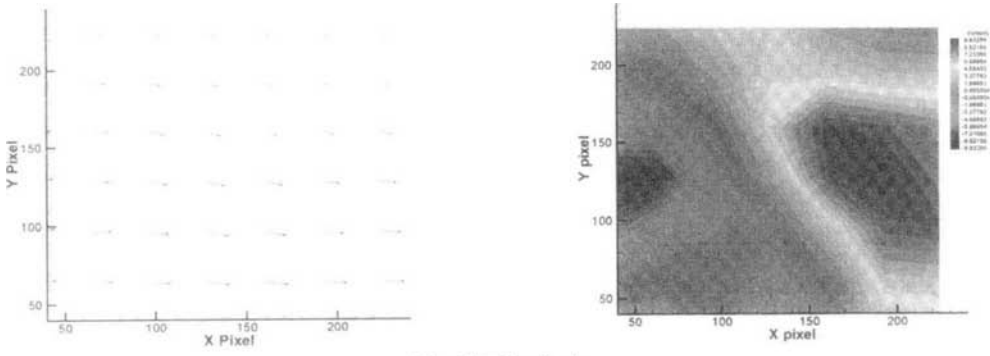
The two-frame PTV method has a little bit lower recovery ratio for flow images of at higher particle concentration. This results from the extra large number of particles which make the match probability calculation difficult to converge.

From the viewpoint of recovery and error ra-

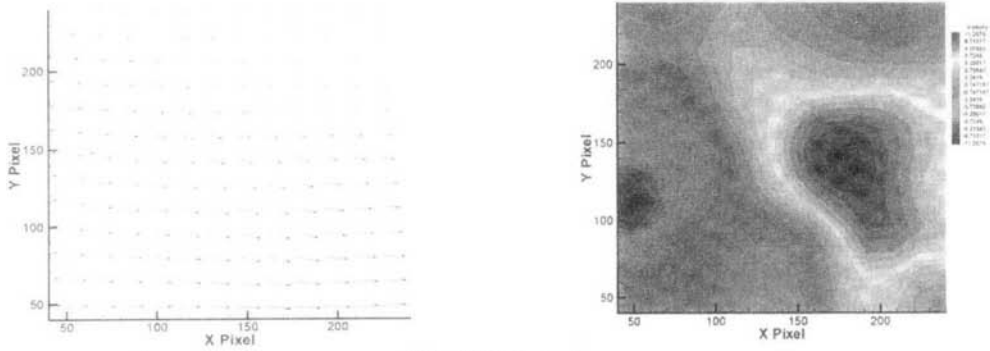
tios, we can see that, when the particle displacement is small and the particle density is high in PIV images, the recursive PIV algorithm shows good performance with satisfied recovery ratio even at small interrogation window. However, for the particle images with lower particle density and larger particle displacement, the performance of recursive PIV method at smaller IW size is influenced by increase of the number of error vectors and reduces the efficiency of the algorithm.

3.3 Standard PIV images

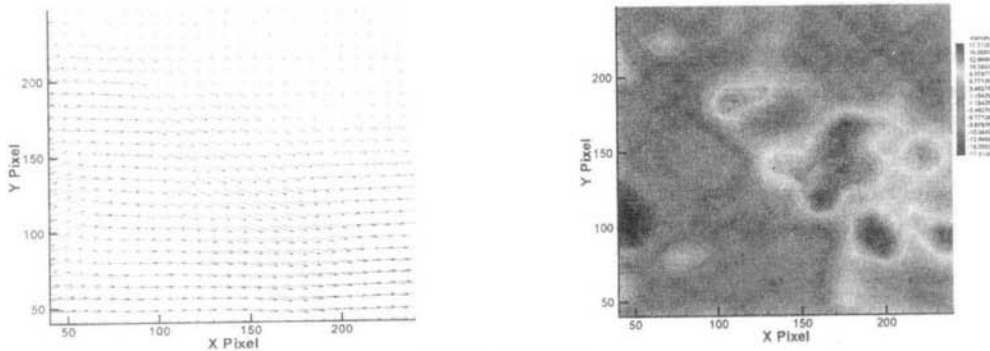
Visualization Society of Japan (VSJ) provides the Standard PIV images generated by numerical simulation to evaluate the effectiveness and accuracy of PIV programs. In this study, the standard PIV image of impinge jet flow was used to test the performance of the recursive PIV correlation algorithm. The resolution of flow image is 256×256 pixels with $N=4000$ particles and 5 pixels of average particle diameter. Figure 7 represents the variation of velocity field and vorticity distribution of the impinging jet by varying IWsize. Figure 7(a) shows the results of the PIV correlation method based on conventional FFT at the first level of spatial resolution of 64×64pixels IW size. As the interrogation window size decreases recursively to 32×32 pixels and 16×16 pixels, it gives more detailed flow structure and precise vorticity distribution with enhanced spatial resolution. With decreasing interrogation window size, the maximum value of vorticity is also increased from reduction of smoothing effect at large interrogation window. The recursive PIV results for 8×8 pixels IW size show much fine



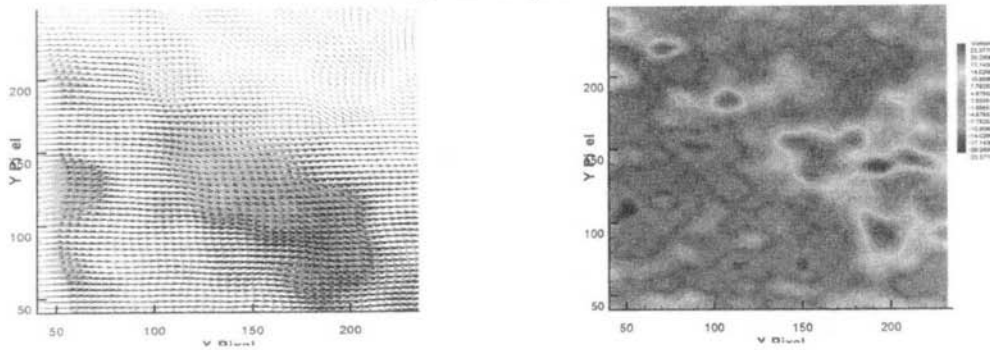
(a) 64x64 pixels



(b) 32x32 pixels



(c) 16x16 pixels



(d) 8x8 pixels

Fig. 7 Variation of velocity field and vorticity contours for standard PIV image

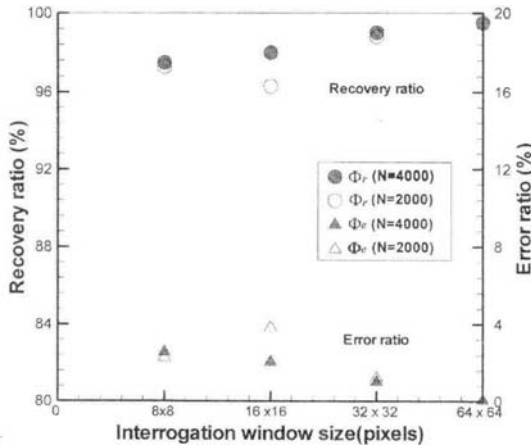


Fig. 8 Variations of recovery ratio and error ratio for the standard PIV images (maximum displacement : 15 pixels)

vortex structure from the same particle images, compared with only 2 or 3 vortices for the case of 32×32 pixels. For the standard image with $N=4000$ particles, the minimum Φ_r is about 97.5% and the maximum Φ_e is about 2.56% at the smallest IW 8×8 pixels. Therefore, appropriate compromise is needed in determining the interrogation window size in consideration of increasing spatial resolution and error ratio.

The recovery ratio Φ_r and error ratio Φ_e for the standard PIV images containing $N=2000$ and $N=4000$ are compared as a function of interrogation window size for the maximum displacement of 15 pixels and the results are shown in Fig. 8. With increase of the interrogation window size, the recovery ratio Φ_r is increased and the error ratio Φ_e is decreased for both cases. With decrease of number of particles (N), Φ_r is increased and the error ratio Φ_e is decreased. For the large value (15 pixels) of maximum displacement, if the number of particles is less than 2000, Φ_r decreases rapidly and the Φ_e increases largely for the small interrogation window (The result is not shown here). If the flow images have sufficient particle density, the recovery ratio can be close to 100% and Φ_e reaches 0% for higher recursive steps. Though the recursive correlation algorithm improves the spatial resolution remarkably, densely seeded particle images with small particle

displacement are needed to get sufficient recovery ratio and avoid loss of flow field information.

3.4 Real flow applications

The performance of the recursive correlation PIV technique was evaluated for two different real flows ; (1) ventilation flow in a vehicle passenger compartment, and (2) wake flow behind a circular cylinder with riblet surface.

3.4.1 Ventilation flow in a passenger compartment

Particle images of the ventilation flow inside a vehicle passenger compartment model were captured with a high-resolution CCD camera of $2K \times 2K$ pixels. The details of the experimental apparatus were described by Yoon and Lee (1998). Figure 9 shows the velocity fields for the flow behind the front seat of vehicle at three different spatial resolution levels of 64×64 pixels, 32×32 pixels and 16×16 pixels IW sizes. The velocity field was extracted from the entire velocity vector map. For IW of 64×64 pixels, only large-scale flow motions can be observed and the vortex at the lower right corner just behind the front seat is hardly identified. By increasing the spatial resolution to the second level of 32×32 pixels interrogation window, the PIV results reveal the detailed flow structure and vortical distribution with enhancement of spatial resolution. The outline of the vortex at down right corner is distinguished clearly and the maximum value of vorticity is increased about 70%. As the interrogation window size is further decreased to 16×16 pixels, the vorticity field shows that the large-scale vortex structures are composed of many small-scale vortex structures and velocity field provides more subtle turbulent flow motion. The value of maximum vorticity is about 50% higher than that of 32×32 pixels IW due to reduction of smoothing effect encountered in larger interrogation window.

3.4.2 Wake behind a circular cylinder with riblet surface

The near wake behind a circular cylinder with riblet surface is different from that of a smooth

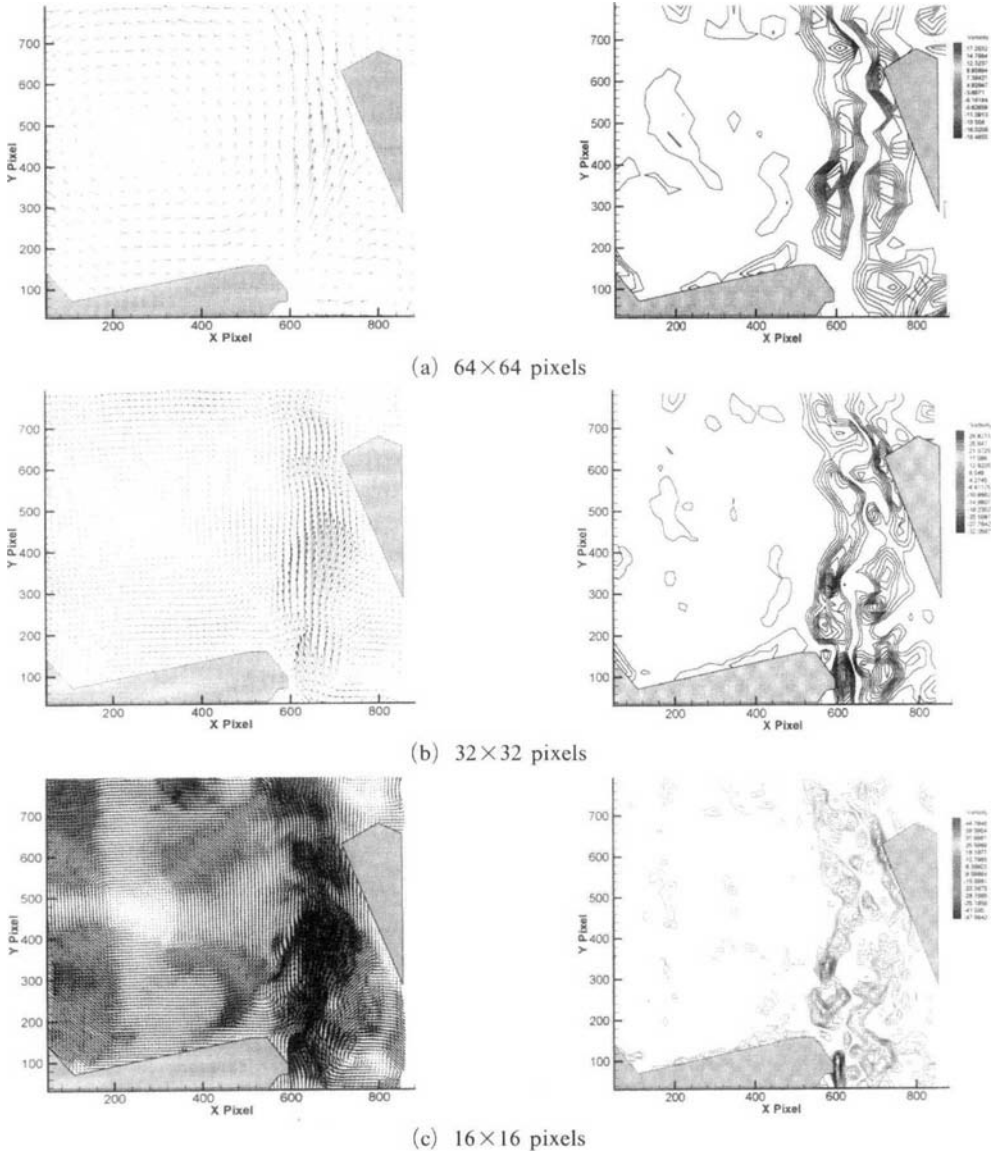


Fig. 9 Velocity fields and vorticity contours of Ventilation flow in a vehicle passenger compartment

circular cylinder. The drag force acting on the riblet-surfaced cylinder is reduced compared with that of a smooth cylinder. The PIV measurements were carried out in a circulating water channel having a test-section of $0.3\text{ m}^w \times 0.25\text{ m}^h \times 1.5\text{ m}^l$. A circular cylinder of $D=20\text{ mm}$ in diameter was mounted horizontally in the test-section and the field of view was $60\text{ mm} \times 60\text{ mm}$ just behind the cylinder. The Reynolds number based on the cylinder diameter was about $Re=3000$. The PIV results were obtained for three different IW sizes

of 64×64 , 32×32 and 16×16 pixels. The resulting velocity fields and vorticity distributions are shown in Fig. 10. The cylinder is located at the left edge in the velocity maps. At the spatial resolution level of 64×64 pixels, the obscure outlines of large-scale vortices are observed. As the spatial resolution is improved to the second level of 32×32 pixels, the position of vortex shedding is distinguished clearly and a clockwise-rotating small-scale vortex structure is also revealed. The vortex shedding procedure becomes

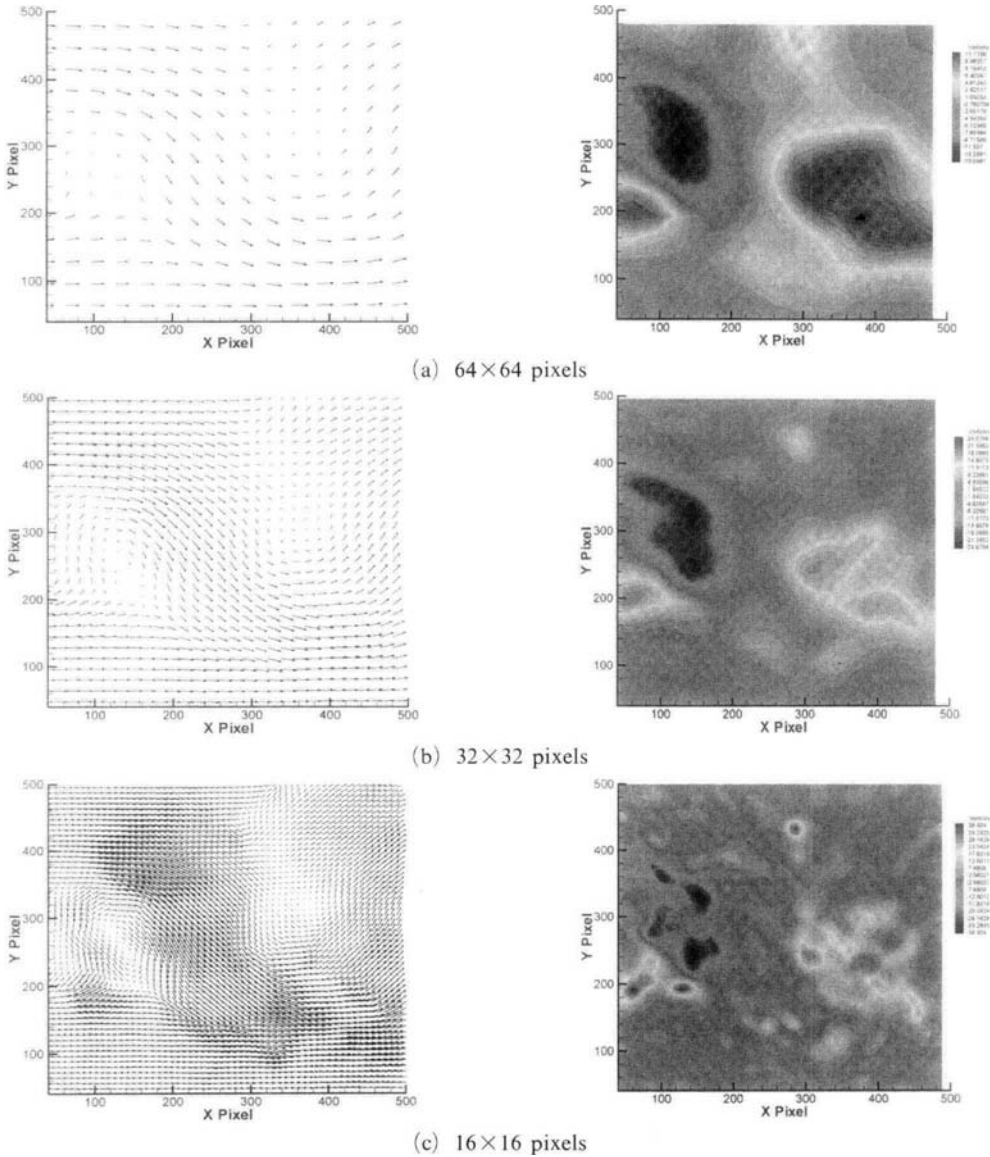


Fig. 10 Velocity fields and vorticity contours of near wake behind a circular cylinder with riblet surface

much clear when the spatial resolution is further increased to the higher level of 16×16 pixels.

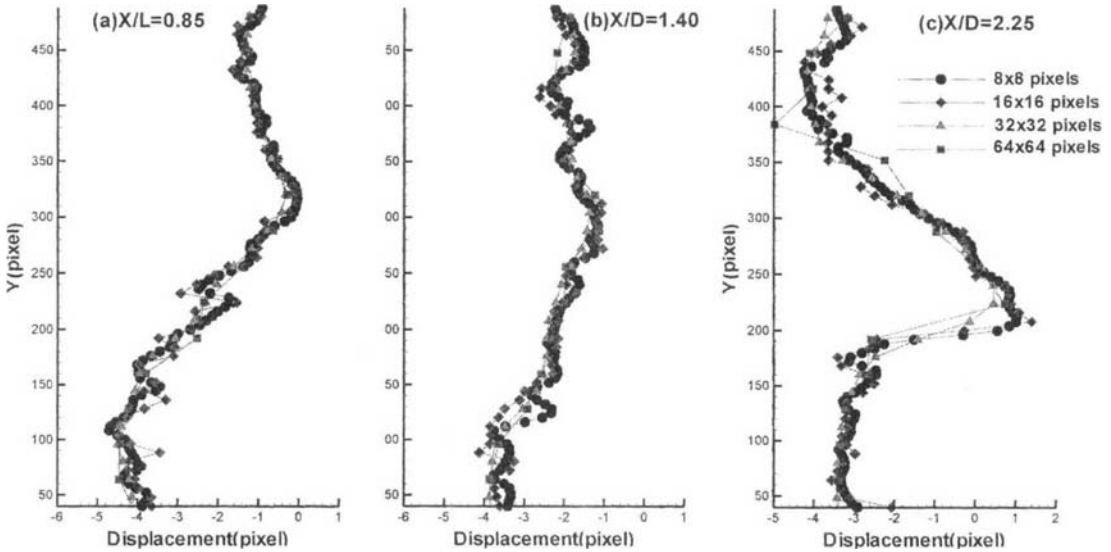
Figure 11 shows the quantitative comparison of stream-wise velocity profiles at downstream locations of $X/D=0.85, 1.40$ and 2.25 extracted from the PIV velocity field results for different spatial resolution levels. The magnitude of PIV result is enhanced in principle with increase of spatial resolution level, it indicates that the sub-pixel accuracy is improved. However, at the window size of 16×16 pixels, the velocity profiles show

some fluctuations. This maybe attribute to decrease of SNR (signal-noise ratio) on correlation plane. From this result, we can see that the recursive PIV algorithm should be employed with preliminary evaluation of performance in advance to find out the optimal spatial resolution for given particle images.

When many instantaneous velocity fields are ensemble averaged to calculate the spatial distribution of turbulence statistics, the decrease of computation time becomes of great importance.

Table 2 Comparison of total computation time for the recursive PIV algorithm

Image size (pixel)	Number of recursion	Interrogation window size (pixel)	Number of interrogation windows	Total computation time (Sec.)
512×512	0	64×64	196	2
	1	32×32	784	4
	2	16×16	3136	11
	3	8×8	12544	29

**Fig. 11** Comparison of stream wise velocity profiles for various spatial resolution levels

For the case of PTV method, the particle density for a given flow significantly affects the computation time required for tracking correct velocity vectors. However, for the PIV method, the computation time is mainly affected by the captured image size in pixels, the interrogation window size and the overlapping ratio. For the comparison of total computation time, the particle images (512×512 pixels) of flow behind a circular cylinder having riblet surface are calculated using a PC with Intel Pentium Celeron 800 CPU and 256 MB memory. The computation times elapsed to recover the correct velocity vectors are compared with varying the IW size and recursive steps. For each recursive PIV processing step, the overlapping ratio of the adjacent IW is fixed to 50%. The results are summarized in Table 2. Though the smallest IW of 8×8 pixels provides large number of velocity vectors and improves the

spatial resolution of flow field, the total computation time and the error ratio are largely increased. For the real flows tested in this study, the 16×16 pixels IW seems to give the best results in the consideration of spatial resolution, number of error vectors and total computation time.

4. Conclusion

The performance of hierarchical recursive correlation algorithm with CBC processing has been tested using the synthetic particle images, standard PIV images and finally for real flows. Compared with the correlation PIV method based on conventional FFT, the CBC processing suppresses the spurious vectors notably and increased the SNR (signal to noise ratio) on multiplied correlation plane, improving the efficiency of peak detection and sub-pixel accuracy of PIV

measurement. The hierarchical recursive correlation PIV algorithm is found to be very effective in improving the spatial resolution of velocity field results with decrease of interrogation window size. It gives detailed flow structures with increased measurement accuracy. However, the straightforward application of present algorithm on higher level of recursive treatment to sparsely seeded flow or flow with large particle displacement may decrease the recovery ratio of correct vectors. It also influences on the prediction of offset for each interrogation window in the higher level of recursive processing. For the case of ensemble averaging of many instantaneous velocity fields to get the spatial distributions of turbulence statistics, several consecutive adoption of recursive processing will largely increase the total computation time and the number of error vectors. In addition, due to increase of error vectors number, the time for post processing routine is also increased. Therefore, it is recommended to determine the optimal number of recursive processing steps and appropriate interrogation window size in advance to compromise spatial resolution and error vectors for a given sparsely seeded flow.

Acknowledgment

This study was sponsored by NRL(National Research Laboratory) program of the Ministry of Science and Technology, Korea.

References

- Baek, S. J. and Lee, S. J., 1996, "A New Two-frame Particle Tracking Algorithm Using Match Probability," *Experiment in Fluids*, Vol. 22, pp. 23~32.
- Hart, D. P., 1999, "Super-Resolution PIV by Recursive Local-Correlation," *Journal of Visualization*, Vol. 10, pp. 1~10.
- Hart, D. P., 2000, "PIV Error Correction," *Experiments in Fluids*, Vol. 29, pp. 13~22.
- Hu, H., Saga, T., Kobayashi, T., Taniguchi, N. and Segawa, S., 2000, "Improve the Spatial Resolution of PIV Results by Using Hierarchical Recursive Operation," *Proc. 9th Int. Symp. Flow Visualization*, Edinburgh, U.K.
- Kean, R. D. and Adrian, R. J., 1990, "Optimization Particle Image Velocimetry," *Measurement Science and Technology*, Vol. 2, pp. 1202~1215.
- Kim, H. B and Lee, S. J., 2002, "Performance Improvement of Tow-frame Particle Tracking Velocimetry Using a Hybrid Adaptive Scheme," *Measurement Science and Technology*, Vol. 13, pp. 573~582.
- Park, K. H. and Kim, K. C., 2001, "Development of a High Resolution Digital Cinematic Particle Image Velocimetry," *KSME Journal*, Vol. 25, No. 11, pp. 1535~1542. (in Korean)
- Rohaly, J., Frigerio, F. and Hart, P. D., 2001, "Reverse Hierarchical PIV Processing," *Proc. 4th Int. Symp. Particle Image Velocimetry*, Göttingen, Germany.
- Scarano, F. and Riethmuller, M., 1999, "Recursive Multigrid Approach in PIV Image Processing with Discrete Window Offset," *Experiments in Fluid*, Vol. 26, pp. 513~523.
- Scarano, F., 2001, "An Adaptive Resolution Approach in Recursive PIV Image Interrogation," *Proc. PSFVIP-3*, March, 2001, Maui, Hawaii, USA.
- Yoon, J. H. and Lee, S. J., 1998, "Simultaneous Measurement of Temperature and Velocity Fields of Ventilation Flow in a Passenger Compartment," SAE 980292.